ARTICLES

Thermally excited vibrations of the mirrors of laser interferometer gravitational-wave detectors

A. Gillespie and F. Raab
LIGO Project, California Institute of Technology, Pasadena, California 91125
(Received 14 November 1994)

The effect of thermally excited mirror vibrations on length measurements using a laser interferometer gravitational-wave detector is calculated, and the number of vibrational modes which must be included to predict the Brownian motion of the mirror surface relative to its center of mass is estimated. These calculations account for both the full three-dimensional shape of the vibrational modes of the mirrors and the spatial shape of the optical modes of the interferometer. A convergence pattern for the number of modes which must be included in a complete thermal noise estimate is found; all vibrational modes with acoustic wavelengths greater than the laser beam spot size must be considered. When the full geometries of the mirror and the optical mode are taken into account, the thermal noise power in the gravitational-wave frequency bandwidth for mirror and laser parameters relevant to the LIGO (Laser Interferometer Gravitational-Wave Observatory) interferometer is approximately a factor of 6 larger than the noise obtained in earlier estimates which typically considered only the lowest few modes. If mirror vibrational thermal noise was the limiting noise source for the detection of some astrophysical sources, then this difference in noise power would result in a factor of 15 difference in estimated detection rates for these sources.

PACS number(s): 04.80.Nn, 05.40.+j

I. INTRODUCTION

Gravitational-wave observatories, such as the Laser Interferometer Gravitational-Wave Observatory (LIGO) [1] and VIRGO [2] facilities now being built, will use laser interferometry to sense the small motions of suspended test masses induced by gravitational waves. To observe signals from astrophysical sources, background motion of the test masses caused by local environmental forces must be minimized. Once background noise from seismic, acoustic, and electromagnetic forces is sufficiently well suppressed, the main background arises from the thermally excited motion of the masses, sometimes referred to as Brownian motion. The motion of the center of mass of the test mass, typically referred to as suspension thermal noise, has been discussed in several recent papers [3–5]. Here we concentrate on the internal vibrations of the test mass, which cause the motion of the mirrored surfaces relative to the centers of mass of the test masses.

We have developed a method for calculating the optical path length changes induced by mirror vibrations and predicting the spectral distribution of noise in the interferometer due to thermally driven vibrations [6] (see also [7]). Here we present this analysis and its implications in detail. Previous estimates [8,9] of the thermal noise in laser interferometers have only included the lowest few vibrational modes of the mirrors and have estimated the coupling between the vibrations of the mirror and the optical path length by only considering purely longitudinal motion. In the calculations presented below, the mirrors are treated as three-dimensional bodies, and a convergence pattern for the number of modes needed to describe the thermal noise accurately is found. The vibrational thermal noise of the LIGO project's first generation full-scale interferometer and 40-m interferometer at Caltech are investigated as examples; however the method is general and can be applied to any interferometer with suspended mirrors. We find both that more modes must be considered to estimate the thermal noise accurately and that many modes are more strongly coupled to the interferometer than was previously thought. The result is that the thermal noise due to mirror vibrations is larger than previously estimated and may limit the sensitivity of advanced gravitational-wave detectors.

Following Saulson [9], we assume that the losses in the substrate material are independent of frequency. We believe this assumption to be consistent with current experimental results in fused silica [10], the preferred test mass material for both optical and mechanical reasons. Our method of calculation is independent of the specific loss function chosen, but the absolute level of the estimate of thermal noise is sensitive to the loss function.

The effect of mirror vibrations on the optical mode of an interferometer and the implications for length measurements are treated in Sec. II. We define a single parameter for each vibrational mode of the test mass, the effective mass coefficient, which can be used to parametrize this interaction. Our method for calculating these coef-

ficients was verified as described in Sec. III. Section IV describes how thermal noise in an interferometer is calculated as a summation over test mass modes and Sec. V explains how physical parameters of the interferometer affect the convergence of this sum. The sensitivity of these thermal noise estimates to the position of the optical mode on the mirror is investigated in Sec. VI. Section VII discusses how the results of these calculations can be used to estimate thermal noise in real mirrors, where deviations from perfect symmetry may cause mixing of the vibrational modes. The implications of this work for gravitational-wave detectors are discussed in Sec. VIII.

II. EFFECT OF MIRROR VIBRATIONS ON OPTICAL MODES OF AN INTERFEROMETER

The initial LIGO interferometer [1], shown schematically in Fig. 1, will consist of suspended mirrors forming Fabry-Perot optical cavities. The cavities are arranged along orthogonal axes to sense the strain induced by passing gravitational waves. The strain is manifested as apparent displacements of the cavity mirrors, detected by laser light which resonates in the optical cavities. Vibrations of the mirrors constitute a noise background which could mask or mimic a gravitational-wave signal.

We wish to find the displacements detected by the optical system when the mirror surfaces are vibrating. To solve this problem, we must consider the interaction between two different types of modes: the mechanical modes of the vibrating test masses, and the optical modes of the electromagnetic field resonating in the Fabry-Perot cavities.

The vibrational eigenmodes and eigenfrequencies of a free right solid cylinder can be found by solving the equations of elasticity using an analytic series solution [11]. From the results of that solution, the amplitude of the displacement of the mirror surface at each point, $\vec{u}_n(\rho,\theta)$, can be calculated for the nth mode normalized to a fixed energy U. Implicit in the mode shape $\vec{u}_n$ is a time dependence $e^{i\omega_n t}$.

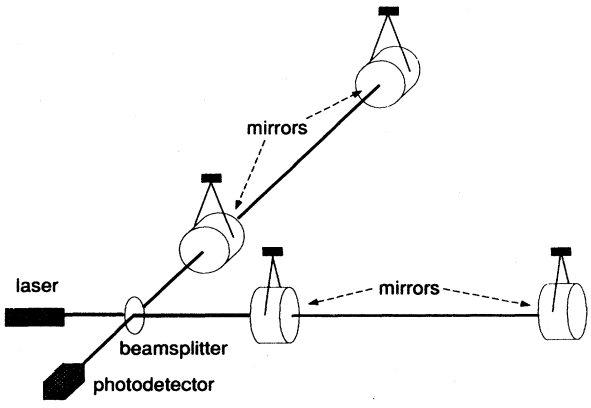

FIG. 1. Schematic view of a LIGO interferometer.

The optical modes of the interferometer can be described by Hermite-Gaussian functions, ψ_{lm} [12]. The interferometer typically operates with the transverse-electromagnetic (TEM_{00}) mode ψ_{00} on resonance. To avoid interference between modes, the length of the interferometer and the curvature of the mirrors are chosen such that the TEM_{00} mode and other higher-order modes cannot resonate simultaneously [13].

The optical mode experiences a phase shift upon reflection from a mirror excited in a particular vibrational mode:

$$\psi_{00}(\rho,\theta,z) \rightarrow \psi_{00}(\rho,\theta,z)e^{i2\vec{k}\cdot\vec{u}_n(\rho,\theta)} \approx \psi_{00}[1 + i2\vec{k}\cdot\vec{u}_n - 2(\vec{k}\cdot\vec{u}_n)^2] \ . \quad (1)$$

$\vec{k}$ is the wave vector, and $|\vec{k}\cdot\vec{u}_n|$ is taken to be much less than unity for all points on the mirror surface. This new perturbed mode in the interferometer can be described in terms of the unperturbed modes:

$$\psi = \sum_i \sum_j c_{ij}\psi_{ij} \ , \quad (2)$$

$$c_{ij} = \int_S \psi_{ij}^* \psi_{00} e^{i2\vec{k}\cdot\vec{u}_n(\rho,\theta)} d\sigma \ . \quad (3)$$

The integral is an area integral over the mirror surface S. Since only the TEM_{00} component of the perturbed light resonates, the new resonating mode can be written as

$$\psi \approx \psi_{00}\left[1 + i2\int_S \psi_{00}^*\psi_{00}\vec{k}\cdot\vec{u}_n d\sigma - 2\int_S \psi_{00}^*\psi_{00}(\vec{k}\cdot\vec{u}_n)^2 d\sigma\right] . \quad (4)$$

Each term of this expression can be easily interpreted. The imaginary term contains the phase shift from which the apparent length change Δl_n can be determined:

$$\Delta l_n = |\vec{k}|^{-1}\int_S \psi_{00}^*\psi_{00}\vec{k}\cdot\vec{u}_n(\rho,\theta)d\sigma \ . \quad (5)$$

The second integral term describes the light which is scattered out of the TEM_{00} mode. The apparent motion Δl_n is generally different for different vibrational modes of the mirror with the same energy.

To remove the dependence of the amplitude of the displacements, $\vec{u}$, on the energy normalization, it is convenient to parametrize the coupling of each mode in terms of an effective mass coefficient α_n defined as

$$\alpha_n = \frac{U}{\frac{1}{2}m\omega_n^2\Delta l_n^2} \ . \quad (6)$$

m and ω_n are the actual mass of the mirror and the angular resonant frequency of the vibrational mode, respectively. With this parametrization, the apparent motion of the illuminated mirror surface oscillating in a particular vibrational mode can be modeled as if it were

a point mass of magnitude $\alpha_n m$ vibrating with a resonant frequency ω_n measured by an ideal one-dimensional laser beam. The result of this mathematical procedure is shown schematically in Fig. 2.

As an example, the mode shapes, resonant frequencies, and effective mass coefficients of the first six axisymmetric modes of a 10-cm mirror are shown in Fig. 3. A 10-cm mirror (used in the LIGO project's 40-m interferometer) is a fused silica cylinder with a diameter of 10 cm, a length of 8.8 cm, and a mass of 1.6 kg. The effective mass coefficients depend not only on the parameters of the mirror, but also on the geometry of the optical mode on the mirror surface. For all the calculations of this paper, except in Sec. V where it is explicitly stated otherwise, the laser parameters used with the 10-cm mirror are those relevant to the 40-m prototype interferometer, which has a spot size (the radius at which the intensity is $1/e^2$ of its maximum) of 0.22 cm. The beam is assumed to be centered on the mirror and in the TEM_{00} optical mode, so that nonaxisymmetric vibrational modes do not contribute apparent motion to the mirror surface. The benefit of this choice of beam location is that the center of the mirror is a node for all nonaxisymmetric modes, making calculations much simpler by decreasing the number of modes involved. The implications of moving the beam spot off center are discussed in Sec. VI.

The effective mass coefficients of the first 100 axisymmetric modes of a 10-cm mirror are plotted against their respective resonant frequencies in Fig. 4. The effective mass coefficients vary by several orders of magnitude, reflecting the wide variety of mode shapes. There is, however, a general trend toward lower effective masses at larger resonant frequencies. To draw attention to this trend, a dashed line representing $\alpha_n \propto f_n^{-1}$ is drawn. This line is approximately the median effective mass coefficient in a given bandwidth. The significance of this line will become apparent in Sec. V. This general trend arises from the cylindrical symmetry of the axisymmetric modes, which dictates that the largest antinode of motion in the axial direction is at the center of the mirror, the position being sampled by the laser. When the acoustic wavelength is shorter, this antinode will have a narrower width and thus a larger amplitude for a given energy. Hence the apparent motion of the mirror surface sampled by the laser light can be relatively larger for the higher-frequency modes, and the effective mass can be correspondingly smaller. To illustrate this point, the shapes of the mirror surface for four modes with small effective masses are shown in Fig. 5 (these modes are shown as solid circles in Fig. 4); notice that a relatively

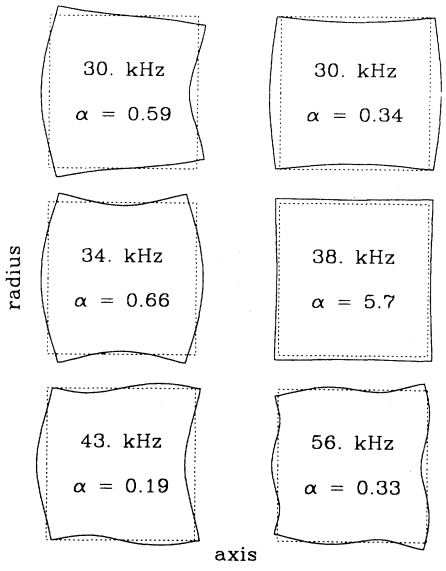

FIG. 3. Mode shapes, resonant frequencies, and effective mass coefficients of a 10-cm mirror.

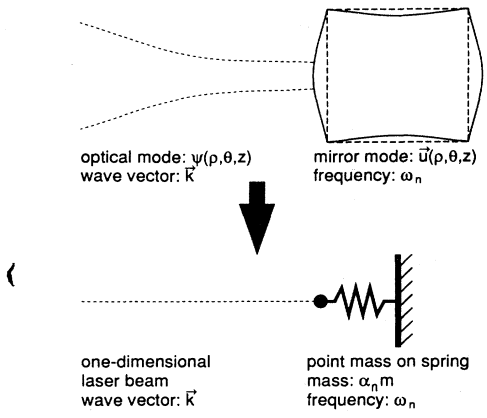

FIG. 2. Representation of the effective mass coefficient. The effective mass coefficient, α, is the parameter which we use to model the interactions between the optical mode of the interferometer and a vibrational mode of the mirror as a one-dimensional mass-spring system.

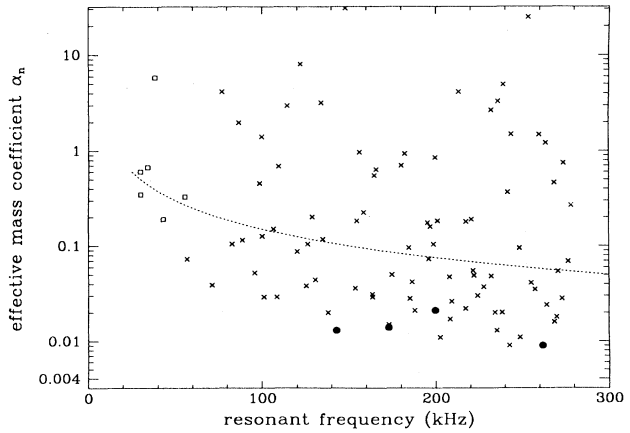

FIG. 4. The effective mass coefficients as a function of mode resonant frequency for a 10-cm mirror. The modes shown in Fig. 3 are plotted as open squares; the modes shown in Fig. 5 are plotted as solid circles. The dashed line corresponds to $1/f$.

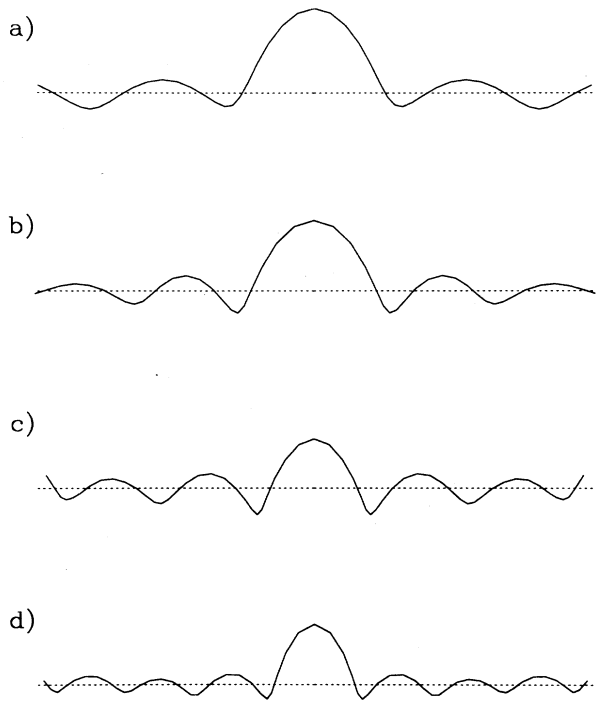

FIG. 5. The shape of the mirror surface for four higher-frequency modes with small effective masses. (a) $f = 143$ kHz, $\alpha = 0.013$; (b) $f = 173$ kHz, $\alpha = 0.014$; (c) $f = 200$ kHz, $\alpha = 0.021$; (d) $f = 262$ kHz, $\alpha = 0.009$.

small portion of the mirror around the center of the mirror surface moves much more than any other spot.

Previous estimates (see, for example, [9]) of the coupling between the vibrational modes of the mirror and the optical path length of the interferometer considered only purely longitudinal motion. In this case the mode shapes can be described simply by

$$u_n(z) = u_0 \sin\left(\frac{n\pi z}{2h}\right) , \tag{7}$$

where h is the thickness of the mirror. Such a model predicts an effective mass coefficient of 0.5 for all modes. This approximation gives a reasonable estimate of the effective mass coefficients of some low-frequency modes (e.g., the first few modes of Fig. 3). However, such a model fails to predict the much lower effective masses of some of the higher-frequency modes that are shown in Fig. 4, and therefore this model underestimates the total noise contributed by mirror vibrations.

To check the self-consistency of our three-dimensional model, the approximations that went into its formulation must be examined. The first assumption is that $|\vec{k}\cdot\vec{u}_n| \ll 1$. This line is approximately the same as requiring that $|\vec{k}|\Delta l_n \ll 1$. Since we are supposing that the vibrations are thermally excited, it follows from the equipartition theorem that

$$\Delta l_n \approx \sqrt{k_B T/\alpha_n m\omega_n^2} , \tag{8}$$

where k_B and T are Boltzman's constant and the temperature, respectively. Hence at a temperature of 300 K, $|\vec{k}| \cdot \Delta l_n$ is of order 10^{-10} for the lower-frequency modes shown in Fig. 3, clearly satisfying the requirement $|\vec{k}\cdot\vec{u}_n| \ll 1$.

The second integral term of Eq. (4) which describes the scattered light is of order 10^{-20} of the light incident on the mirror for the modes of Fig. 3. This is small compared to the constant scattering due to microroughness and figure errors in the mirror, which will be of order 10^{-4}–10^{-6}. However, the amplitude of the light scattered by thermally excited mirror vibrations will be time dependent, and so to estimate its importance we compare its magnitude to another fundamental noise source in the amplitude of the light—the quantum uncertainty of the light power or photon shot noise. An order of magnitude estimate of the frequency bandwidth of the mirror modes (the full width at half maximum of the mirror resonances) is 10^{-3} Hz, and the laser light at the input of the Fabry-Perot cavity is of order 1 W. The corresponding shot noise in the light power at the input mirror is of order 10^{-11} W, whereas the fluctuations in this light due to scattering from mirror vibrations are of order 10^{-20} W. Clearly the scattering term and all higher-order terms of Eq. (4) can safely be ignored.

Another assumption is that the TEM_{00} component of the distorted optical mode reflected from the vibrating mirror surface still resonates in the Fabry-Perot cavity, and that the light scattered into other modes does not. This is true if the change in the resonant frequencies of the optical modes of the cavity due to the vibrations of the mirror is less than the linewidth of the cavity. The frequency shift, $\Delta f = f\Delta l/l$, is of the order of 10^{-3} Hz for the modes of Fig. 3, and the linewidth of the optical cavity under consideration is of order 10^2 Hz, so the light continues to resonate in the primary mode, and modes which were previously separate from the primary mode do not resonate.

III. VERIFICATION OF THE EFFECTIVE MASS COEFFICIENTS

The numerical code used to calculate the effective mass coefficients was subjected to a number of consistency checks. The resonant frequencies were calculated using a FORTRAN code largely provided by Hutchinson. The calculated eigenfrequencies agreed with the theoretical work of Hutchinson [11] and also with the experimental work of McMahon [14] for the appropriate cylinder materials and dimensions. The mode shapes were checked for self-consistency by comparing the elastic energy of deformation in the mode to the kinetic energy in the mode one-quarter of a cycle later:

$$\int_M [\tfrac{1}{2}Ku_{ll}^2 + \mu(u_{ik} - \tfrac{1}{3}\delta_{ik}u_{ll})^2]dV = \int_M \tfrac{1}{2}\rho\omega_n^2\vec{u}\cdot\vec{u}dV . \tag{9}$$

K, μ, δ_{ik}, and ρ are the bulk modulus, shear modulus, Kronecker delta, and the density of the fused silica. The

integral is over the mirror volume M and the displacement vector $\vec{u}$ is now evaluated over the entire mirror volume. u_{ik} is the strain tensor, defined in terms of the displacement vector as

$$u_{ik} = \frac{1}{2}\left(\frac{du_i}{dx_k} + \frac{du_k}{dx_i}\right) . \tag{10}$$

Repeated indices are summed. The effective mass coefficients can also be checked against analytical calculations in the one-dimensional limit where the mirror is made very long and thin [Eq. (7)]. The effective mass coefficients of all modes in this approximation are 0.5. The numerical code passed these basic checks.

A simple experiment was performed to verify directly the calculation of the effective mass coefficients for modes which have acoustic wavelengths much larger than the beam spot size. In this case the laser spot can be approximated by a point. These modes can be driven by gluing a small magnet (with dimensions much smaller than the acoustic wavelength of the mode) to the center of the back of the mirror, which by symmetry has the same effective mass coefficient as the front. Using a Michelson interferometer to measure the mirror's response to forces applied by a current in a coil near the magnet, one can experimentally infer the effective mass of the mode. The apparent motion on resonance is

$$\bar{x} = \frac{Q_n}{\alpha_n m \omega_n^2}\bar{F} , \tag{11}$$

where $\bar{x}$ and $\bar{F}$ are the root-mean-squared displacement and force, and Q_n is the mechanical quality factor of the resonance. The force is proportional to the current, I, through the drive coils; therefore

$$\alpha_n \propto \frac{Q_n}{m\omega_n^2}\frac{\bar{I}}{\bar{x}} . \tag{12}$$

Such an experiment was carried out using one of the 10-cm mirrors, investigating the first five modes of Fig. 3. The resonant frequencies were found to agree with the calculation within 2%; the mirror had a wedged shape for optical reasons which made the thickness of the mirror ill defined at the 1% level. Figure 6 shows a comparison of the measurement of the effective mass coefficients for these five modes to the values of α_n calculated using Eq. (12). The line on the figure indicates a fit to a direct proportionality (the current to force ratio was not calibrated independently). Figure 6 indicates that the effective mass coefficients are an accurate way to model the vibrational modes of a mirror, and that the numerical code used in the calculations was functioning properly.

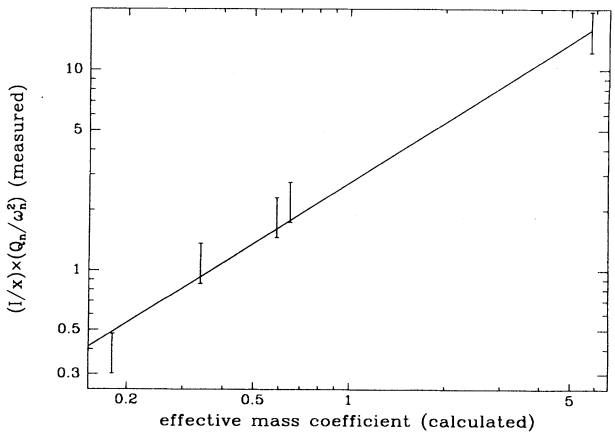

FIG. 6. Comparison between calculated effective mass coefficients and the measured coefficients. The solid line is a direct proportionality.

IV. SPECTRAL DENSITY OF THE THERMALLY EXCITED MOTION

The root-mean-squared motion of a mode of the thermally excited mirror can be calculated using the equipartition theorem as in Eq. (8). At a temperature of 300 K, Δl_n is of order 10^{-16} m for the lowest-frequency modes shown in Fig. 3. As a first approximation, most of the energy of the motion occurs within a bandwidth, Δf_n, around the resonant frequency, f_n, defined by the Q of the mode ($\Delta f_n = f_n/Q_n$). To get a more complete prediction of the spectral density of the motion, the fluctuation-dissipation theorem must be used [9,15]. The vibrational mode is modeled as a harmonic oscillator with a complex spring constant:

$$-\alpha_n m\omega^2\tilde{x} + \alpha_n m\omega_n^2[1 + i\varphi_n(\omega)]\tilde{x} = \tilde{F}, \tag{13}$$

where the dissipation is parametrized by the imaginary part of the spring constant and can, in general, be frequency dependent. We refer to $\varphi_n(\omega)$ as the loss function because the fraction of energy lost in one cycle of oscillation at frequency ω is $2\pi\varphi(\omega)$. The value of the loss function at the resonant frequency is related to the Q of the mode by $\varphi_n(\omega_n) = 1/Q_n$. From the equation of motion (13) and the fluctuation-dissipation theorem, the general spectral density of displacement due to thermal excitation of the nth mode can be derived [9]:

$$S_{xn}(f) = \frac{4k_BT}{\alpha_n m\omega}\left[\frac{\omega_n^2\varphi_n(\omega)}{(\omega^2 - \omega_n^2)^2 + \omega_n^4\varphi_n^2(\omega)}\right] . \tag{14}$$

In this form, the spectral density is implicitly a function of the frequency f in that the motion is described over the usual 1 Hz bandwidth; however the function is written explicitly in terms of the angular frequency, $\omega = 2\pi f$. (This notation, although perhaps initially confusing, simplifies the equation in that it eliminates an abundance of 2π's.) The frequency band of interest for earth-based gravitational-wave detectors (10 Hz to 10 kHz) is generally well below the resonant frequency of the lowest vibrational mode of the mirror, in which case the total thermal noise can be approximated by

$$S_x(f) \approx \sum_n \frac{4k_BT}{\alpha_n m\omega_n^2}\frac{\varphi_n(\omega)}{\omega} . \tag{15}$$

All of the parameters of Eqs. (14) and (15) can be readily measured or calculated except the loss function. We infer an approximate value of $\varphi_n(\omega)$ from the results of several recent measurements. Measuring the loss function for a system with low dissipation can be extremely difficult. What one generally relies on are measurements of the loss function at the resonant frequency and some dissipation model which predicts the general frequency dependence. Q values of order 10^7 have been measured for the vibrational resonances of the 10-cm mirror. Furthermore fused silica oscillators with Q's of order 10^7 and resonant frequencies ranging from 1 Hz to 10 kHz have been built [10]. These results all give a $\varphi_n(\omega_n)$ which is of order 10^{-7} and approximately independent of the resonant frequency. If one assumes that the loss function is the same for all of these modes, then these results are consistent with a loss function of fused silica of $\varphi(\omega) \approx 10^{-7}$, independent of frequency. We adopt this value of $\varphi(\omega)$ for the purpose of estimating thermal noise for the remainder of this paper.

Our estimate of φ should not be taken as either the fundamental level or frequency dependence of the dissipation of fused silica, which is unknown at frequencies near 100 Hz and at room temperature, but rather a summary of what has been observed thus far. The dissipation depends on both the purity and the preparation of the sample, and there is no strong reason to believe that the dissipation could not be reduced if sufficient care were taken.

V. ADDITION OF MODES

The total thermally excited motion of the mirror surface at a given frequency can be predicted from the sum of Eq. (15). This raises the question of how many modes must be counted in the sum to achieve an accurate estimate of the thermal noise. Figure 7 shows the cumulative contribution to the thermal motion at 100 Hz from the first 100 axisymmetric modes for the 10-cm mirror, taking $\varphi(100\ \text{Hz})$ to be 10^{-7} for all modes. The line indicates the cumulative contribution of all modes with resonator frequency less than f, and the $\times$'s indicate the individual contribution of each mode. The contribution of each individual mode decreases with resonator frequency due to the ω_n^2 term in the denominator of Eq. (15), but the mode density increases linearly with frequency (the axisymmetric modes form a two-dimensional system). Also, there is a general decrease in the α_n terms in the denominator in Eq. (15). The result is a cumulative contribution which increases almost linearly with the maximum resonant frequency included. The approximate dependence of the effective mass coefficients on the resonant frequency needed to give this relation is $1/f$, plotted as the dashed line in Fig. 4. More than 100 modes were not included because of numerical precision errors in the series solving the equations of elasticity when more terms were added.

The thermal motion of the mirrors does not actually diverge, but convergence of the series depends upon the beam spot size. As an example, the initial LIGO interferometers will use mirrors with a diameter of 25 cm, a thickness of 10 cm, a mass of 10 kg, and a spot size of 2.2 cm on the vertex mirrors (the mirrors closest to the beam splitter). Figure 8 shows the convergence for an initial LIGO vertex mirror at 100 Hz with the same dissipation as in Fig. 7. Figure 8 also shows the convergence for a 10-cm mirror with the same 2.2-cm size spot. The dot-dashed vertical lines on the figure indicate the frequencies at which half an acoustic wavelength becomes equal to the diameter at which the laser beam intensity is $1/e$ of its maximum. At this frequency the displacement of the modes, $\vec{u}(\rho, \theta)$, begins to cancel in the phase integral of Eq. (4), resulting in larger effective masses

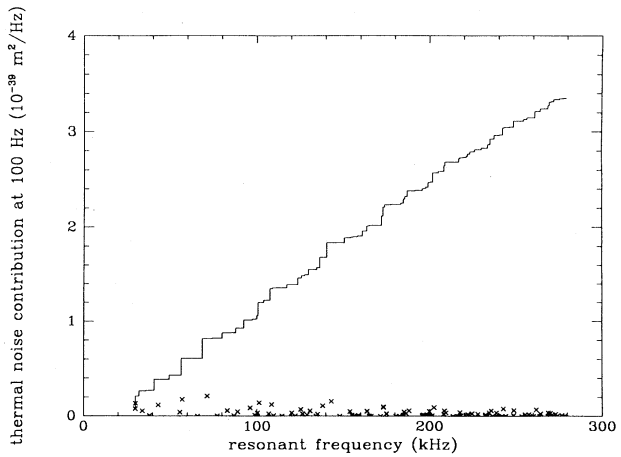

FIG. 7. The contribution to the low-frequency thermal noise of the modes of the 10-cm mirror with a 0.22-cm beam spot. The line is the cumulative contribution and the $\times$'s are the individual contribution of the modes.

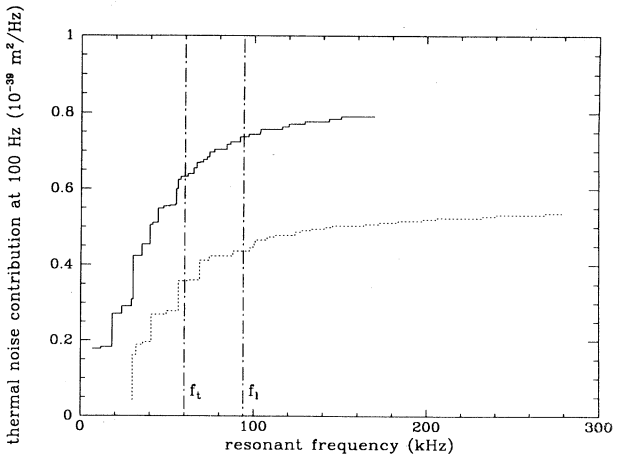

FIG. 8. The cumulative contribution to thermal noise of both the 10-cm (dotted line) and the LIGO 25-cm (solid line) mirrors with a 2.2-cm beam spot. The vertical dot-dashed lines indicate the frequencies at which an acoustic wavelength is of order the beam spot size for both transverse (left line) and longitudinal (right line) waves.

and smaller contributions to the thermal noise. The first vertical line applies to transverse acoustic waves, and the second applies to longitudinal acoustic waves. Each mode is a combination of both transverse and longitudinal motion, and the sum levels off in the region between those two frequencies.

The thermal noise has the following pattern of convergence: the contribution increases approximately linearly with the largest resonant frequency included until the laser beam spot diameter becomes comparable to half an acoustic wavelength. At that frequency the thermal noise sum levels off. In all, of order 100 or more (depending on the geometry of the mirror) modes must be included in order to describe the thermal noise accurately; this number if far more than the few modes used in previous simpler models. Once this pattern of convergence was established, it was verified numerically for several mirror and spot size combinations.

Figure 8 also indicates that mirrors of different geometries can have significantly different thermal noise levels. Typically more modes can contribute to thermal noise for larger mirrors and fewer modes can contribute for larger spot sizes. One should be cautioned, however, that the 10-cm mirror would be inappropriate for use in a full scale (km length) interferometer. Since the radius of the prototype mirror is only twice the spot radius, the optical loss at the edge of the mirror would be too great. Also, in determining the shape of the mirrors one must consider that the light passes through the vertex mirrors; therefore the optical loss in fused silica could restrict the allowed thickness of the mirrors. Optical requirements thus give additional constraints on the geometry of the mirrors.

The convergence pattern of the sum in Eq. (15) is independent of the loss function as long as all of the modes have the same loss function. This is because the relevant parameter for predicting the thermal noise is the loss function evaluated at the frequency of interest, in our case 100 Hz, and not the Q of the resonance, which could depend on the resonator frequency for an arbitrary loss function. The linear increase in the low-frequency thermal noise as more modes are included does depend somewhat on the geometry of the mirror in that the axisymmetric modes are a two-dimensional system. To meet this criterion, both the mirror diameter and its thickness must be greater than the laser spot size. This criterion is met in most realistic applications.

VI. EFFECTS OF MOVING THE BEAM OFF CENTER

The numerical calculations described in the previous sections assumed that the laser was in the TEM_{00} mode and was centered on the mirror. This configuration puts the resonant spot at an antinode of all axisymmetric modes and a node of all nonaxisymmetric modes. By moving the beam off center, the contribution of the axisymmetric modes is decreased and the contribution of the nonaxisymmetric modes is increased. Figure 9 shows

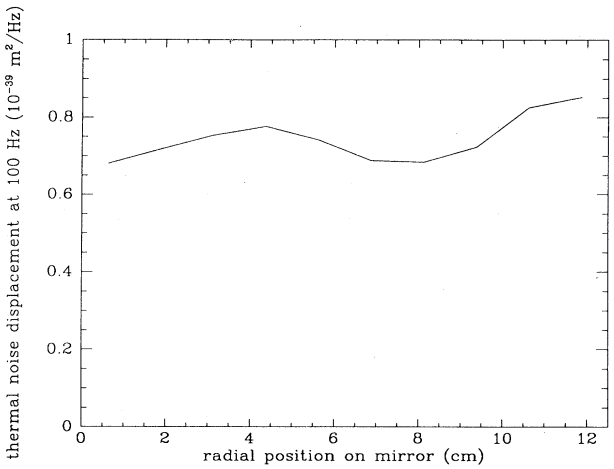

FIG. 9. The thermal motion of a LIGO 25-cm mirror as a function of position on the mirror with 420 modes included.

the effect of moving the beam off center on the LIGO 25-cm mirror. 420 modes with circumferential order (number of nodal lines across the center; axisymmetric modes are order 0) of up to six were included, 60 modes each of circumferential order 0, 1, 2, 3, 4, 5, and 6. These modes included most of the modes with resonant frequencies below 100 kHz (approximately the maximum frequency at which one-half an acoustic wavelength is equal to the spot diameter). The thermal noise is computed using the same parameters as in Sec. V (the laser beam spot size was 2.2 cm). Numerical precision errors prevented more modes from being included; only 60 axisymmetric modes were included to avoid giving those modes too much weight.

The figure shows that except for spots quite near the edge, the thermal noise estimate is relatively insensitive to the exact location of the beam. The thermal noise power varies by 13% across the face of the mirror (an amplitude variation of only 6%). Since the motion of any spot on the mirror surface contains different contributions from each of the mechanical modes, the motion sampled by the light appears to be insensitive to exactly which combination of modes is sampled. It is not clear whether the small variation seen across the mirror surface is real or whether it is an effect of including only a finite number of modes. We hypothesize that if all modes were included, then once the laser beam is more than a few spot diameters (or few acoustic wavelengths of the highest-frequency resonator modes) from the edge of the mirror, the mirror surface would effectively appear to the laser to be an infinite plane with all points having similar amounts of motion. Other interferometer details, such as noise in the alignment of the mirror [16], are likely to put much more stringent requirements on the positioning of the beam on the mirror.

VII. APPLICABILITY OF RESULTS TO REAL MIRRORS

Actual interferometer mirrors differ from ideal right solid cylinders. As mentioned in Sec. III, the mirrors

are wedge shaped for optical reasons. The surface might also be slightly curved. The mirrors are not completely free but are suspended as pendulums by fibers. To define the point of contact between the fiber and the mirror and to prevent rubbing, there may be attachments glued to the mirror, shown in Fig. 10. Furthermore, in order to apply forces to control the orientation of the mirror or to keep the TEM_{00} optical mode on resonance in the interferometer, there may be magnets attached to the mirrors.

These differences can be described as perturbations to shape and boundary conditions of a right solid cylinder. Such perturbations can cause mixing of the modes [17], making the effective mass coefficients difficult to calculate. This problem becomes particularly severe for modes with high resonant frequencies, where the mode density is large (the mode density increases as the resonant frequency squared for a three-dimensional system). However, the results of Sec. VI indicate that the total thermal noise at low frequencies is relatively insensitive to the exact position of the laser on the mirror, or, put another way, the noise power is insensitive to exactly which combination of modes is sampled. Therefore we believe that it is reasonable to expect that the effects of such perturbations cancel when summed over a large number of modes so that the unperturbed calculation is expected to give a good approximation to the total noise power at frequencies far from the mechanical resonances.

Not only will the mechanical modes of the mirror differ from those calculated here assuming an ideal right cylinder, but also the optical modes of the Fabry-Perot cavity will differ from ideal Hermite-Gaussian optical modes. These deviations will be primarily caused by imperfections of the mirror surface. Such perturbed optical modes can be described in terms of their own orthonormal basis or can be expanded in terms of the Hermite-Gaussian orthonormal basis, and then the formalism outlined here can be used to estimate the thermal noise. The effect of a distorted optical mode would be to adjust the effective mass coefficients of the axisymmetric mechanical modes and, if the distortion were not cylindrical, to allow other mechanical modes to couple to the optical path length. Once again, we believe that since our results are insensitive to which modes are sampled, there would not be a strong dependence of the thermal noise power on the optical mode shape.

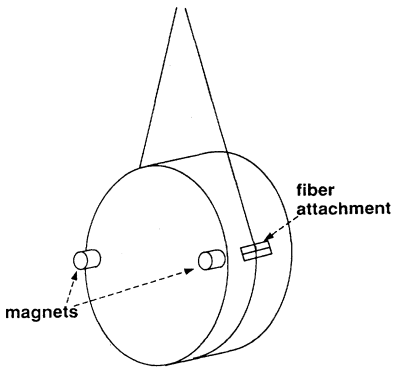

FIG. 10. Schematic view of a mirror with fiber attachments and magnets.

Attachments can also add dissipation to the system and may decrease the Q's of the mirror by large factors. This additional dissipation may affect each mode differently and can be frequency dependent. An example of such a dissipation mechanism which has been studied in detail is resonant coupling between a suspended cylinder and its suspension wires [18]. Any additional damping mechanism which affects each mode differently in some systematic manner will alter the convergence pattern of Sec. V. The additional dissipation from attachments can likely be minimized by using careful experimental technique. These and other surface losses will generally cause less additional dissipation in mirrors which have larger ratios of volume to surface (or contact) area, such as those to be used in the full scale interferometers.

VIII. CONCLUSION

We have developed a detailed model of the thermally excited vibrations of an interferometer mirror. The coupling of each mode to the interferometer has been explicitly calculated, and a convergence pattern determining the number of modes which must be included in the model has been found. Because the coupling between mirror vibrations and optical path length is quite strong for certain high-order vibrational modes, all modes with acoustic wavelengths greater than the laser spot diameter must be considered for an accurate estimate of the thermal noise.

This new estimate of the thermal noise level indicates that vibrational thermal noise may affect the sensitivity of advanced laser interferometer gravitational-wave detectors. The noise level shown in Fig. 8 for a LIGO 25-cm mirror, corresponding to a displacement noise of 5×10^{-20} m/$\sqrt{\text{Hz}}$ or a strain noise of 1.3×10^{-23} $\text{Hz}^{-1/2}$ at 100 Hz with all four mirrors included, lies between the "initial" and "advanced" detector noise levels of [1]. Vibrational thermal noise was not included in [1] because it was previously believed that this noise could be made smaller than other noise sources in the detectors.

This method of estimating the noise can be compared to previously used methods which did not account for the geometry of the mirror or the laser beam. For direct comparison we take Saulson's example [9], which considered a mirror 10 cm in radius and 16 cm thick. This mirror has approximately the same mass as the LIGO 25-cm mirror. Saulson chose the length and radius to minimize the thermal noise from the two lowest-frequency modes. $\varphi(\omega)$ was assumed to be 2.5×10^{-7} and independent of frequency. Saulson's thermal noise estimate, using only the two lowest-frequency modes and assuming an effective mass coefficient of 0.5, was (using his units) $S_x(f) = (2.5 \times 10^{-34}\ \text{cm}^2) \times (1/f)$ [19]. Applying our method of calculation and using his parameters, along with the LIGO laser spot size of 2.2 cm, we arrive at $S_x(f) = (1.5 \times 10^{-33}\ \text{cm}^2) \times (1/f)$. (This thermal noise level, when adjusted for the differing loss functions, is

within 25% of the thermal noise estimate for the LIGO 25-cm mirror; in addition to thermal noise requirements, optical and fabrication considerations determined the geometry of the LIGO mirror.)

This more accurate model gives a thermal noise power that is larger by about a factor of 6. The significance of this factor can be determined by comparing the internal vibrational thermal noise levels to other noise sources and by determining the change in the expected event rate. Saulson's estimate for the internal vibrational thermal noise was slightly above the published "advanced" LIGO noise goals. However, if one assumes a more optimistic loss function which has been achieved in some samples (3×10^{-8}) [20], then the resulting vibrational thermal noise level would be approximately the same as the "advanced" LIGO goals. The extra factor of 6 in noise power that results from our more complete calculation changes the level of vibrational thermal noise from being near the "advanced" detector goals to being significantly above the "advanced" detector goals. If vibrational thermal noise limited the sensitivity to a particular gravitational-wave source, and this calculation indicates that it might, then a factor of 6 in noise power would result in a reduction in the event rate by a factor of 15.

The noise levels discussed here should not be taken as the final estimate of thermal noise, but they do indicate that the goals of the "advanced" interferometers likely require test masses with lower dissipation than was previously thought. The estimate of the dissipation, $\varphi(\omega)$, of 10^{-7} at 100 Hz was based on several recent experiments and reflects the levels of dissipation which have already been achieved. Data obtained so far probably do not represent the fundamental level of dissipation in fused silica, which is unknown. Meeting the thermal noise goals of advanced gravitational-wave detectors will require a better understanding of the dissipation in fused silica (or developing a better mirror material) and an improvement in the loss over what has been achieved thus far.

ACKNOWLEDGMENTS

We thank the entire LIGO team for their encouragement and cooperation. In particular T. Lyons, L. Sievers, and S. Whitcomb provided useful insight. We are especially grateful to J. Hutchinson, who provided the software which calculated the mode resonant frequencies and served as the foundation for these calculations. This work was supported by the National Science Foundation Cooperative Agreement PHY-9210038.

[1] A. Abramovici, W. E. Althouse, R. W. P. Drever, Y. Gursel, S. Kawamura, F. J. Raab, D. Shoemaker, L. Sievers, R. E. Spero, K. S. Thorne, R. E. Vogt, R. Weiss, S. E. Whitcomb, and M. E. Zucker, Science **256**, 325 (1992).

[2] C. Bradaschia, R. Del Fabbro, A. Di Virgilio, A. Giazotto, H. Kautzky, V. Montelatici, D. Passuello, A. Brillet, O. Cregut, P. Hello, C. N. Man, P. T. Manh, A. Marraud, D. Shoemaker, J. Y. Vinet, F. Barone, L. Di Fiore, L. Milano, G. Russo, J. M. Aguirregabiria, H. Bel, J. P. Duruisseau, G. Le Denmat, Ph. Tourrenc, M. Capozzi, M. Longo, M. Lops, I. Pinto, G. Rotoli, T. Damour, S. Bonazzola, J. A. Marck, Y. Gourghoulon, L. E. Holloway, F. Fuligni, V. Iafolla, and G. Natale, Nucl. Instrum. Methods Phys. Rev. A **289**, 518 (1990).

[3] A. Gillespie and F. Raab, Phys. Lett. A **190**, 213 (1994).

[4] G. Gonzalez and P. R. Saulson, J. Acoust. Soc. Am. **96**, 207 (1994).

[5] J. E. Logan, J. Hough, and N. A. Robertson, Phys. Lett. A **183**, 145 (1993).

[6] A. Gillespie and F. Raab, presented at the First International Workshop on Thermal Noise in Laser Interferometer Gravitational-Wave Detectors, Pasadena, California, 1994 (unpublished); A. Gillespie and F. Raab, Bull. Am. Phys. Soc. **39**, 1152 (1994).

[7] F. Bondu and J. Y. Vinet, Phys. Lett. A **198**, 74 (1995).

[8] D. Shoemaker, R. Schilling, L. Schnupp, W. Wrinkler, K. Maischberger, and A. Rüdiger, Phys. Rev. D **38**, 423 (1988).

[9] P. R. Saulson, Phys. Rev. D **42**, 2437 (1990).

[10] V. B. Braginsky, V. P. Mitrofanov, and O. A. Okhrimenko, JETP Lett. **55**, 432 (1992), and references therein.

[11] J. R. Hutchinson, J. Appl. Mech. **47**, 901 (1980).

[12] H. Kogelnik and T. Li, Appl. Opt. **5**, 1550 (1966).

[13] Similar considerations are used in choosing the mirror curvature as were used in A. Rüdiger, R. Schilling, L. Schnupp, W. Winkler, H. Billing, and K. Maischberger, Opt. Acta **28**, 641 (1980).

[14] G. W. McMahon, J. Acoust. Soc. Am. **36**, 85 (1964).

[15] H. B. Callen and T. A. Welton, Phys. Rev. **83**, 34 (1951).

[16] S. Kawamura and M. E. Zucker, Appl. Opt. **83**, 3912 (1994).

[17] J. E. Logan, N. A. Robertson, J. Hough, and P. J. Veitch, Phys. Lett. A **161**, 101 (1991).

[18] J. E. Logan, N. A. Robertson, and J. Hough, Phys. Lett. A **170**, 352 (1992).

[19] This number is corrected from the stated value in [9] of 1.4×10^{-34}, which was in error. [P. R. Saulson (private communication).]

[20] V. B. Braginsky, V. P. Mitrofanov, and S. P. Vyatchanin, Rev. Sci. Instrum. **65**, 3771 (1994).